Investigation of the Performance of Al-Composite developed from Industrial waste: A sustainable perspective

Neeraj Sharma[1], Dharmana Lokanadham[2,a,*] , Rakesh Chandmal Sharma[3,4], Srihari Palli[3,b], K. Venkatasubbaiah[5], B. V. Ramana[6]

1. Production Engineering Department, National Institute of Technology Agartala, Tripura, India (kkrneeraj@gmail.com, +91-9306693726)
2. Mechanical Engineering Department, Aditya Institute of Technology and Management, Tekkali, India ([a]dloknadham@gmail.com, +91-9441914428) [*]Corresponding author ([b]srihari.palli@gmail.com,+91-9985660927)
3. Mechanical Engineering Department, Graphic Era (Deemed to be University), Dehradun, India (rcsharma.me@geu.ac.in, +91-8059930977)
4. Mechanical Engineering Department, Graphic Era Hill University, Dehradun, India
5. Department of Mechanical Engineering, Andhra University, Visakhapatnam, India (profkvsaumech@gmail.com, +91-9848063452)
6. Information Technology Department, Aditya Institute of Technology and Management, Tekkali, India (ramana.bendi@gmail.com, +91-9441053733)

ABSTRACT

The present work aims at developing an Aluminium metal Matrix Composite (AMC) with an industrial waste Lime Stone Powder (LSP) as reinforcement, which is available in plenty at no cost. The main objective of the present study is to investigate the effect of four control parameters viz.: load (L), percentage of LSP reinforcement (R), sliding distance (D), sliding velocity (V) on two tribological properties wear rate (WR) and coefficient of friction (CF) of AMC reinforced with LSP. The composites are manufactured using the stir casting process with varying LSP percentages (0%, 4%, 8%, 12%, 16%). The wear test is conducted using Pin-on-disc apparatus. Taguchi L_{25} orthogonal array design is employed to investigate the effect of the above control parameters on the tribological responses. Analysis of Variance (ANOVA) employment indicates that wear rate depends on sliding distance and load, while the coefficient of friction depends on load and wt.% of LSP. The minimum wear rate of Al-LSP is found to be 0.1952, while the minimum coefficient of friction of Al-LSP determined is 0.0905. To minimize wear rate and coefficient of friction

simultaneously, a composite objective function is created using Grey Relational Analysis (GRA).

KEYWORDS: Al-composite; Grey approach; lime stone powder; wear rate; coefficient of friction.

* *Corresponding author email: dloknadham@gmail.com*

1. Introduction

With technological development, a lot of materials have been developed, and metal matrix composites are one of these developed materials. These materials exhibit different characteristics like wear resistance, high strength, rigidity, etc., making them a good fit for various aerospace and automobile applications. The matrix materials used to develop composite materials are magnesium, aluminium, titanium, etc. Out of there aluminium matrix is mainly used, and the characteristics are improved using various reinforcement like silicon nitride, SiC, TiC, B_4C, Al_2O_3, etc. With the increase in the demand for the aluminium composite, the measurement of its physical, mechanical and tribological characteristics also increases. Researchers developed different techniques to develop the composites, which increase the strengthening of fibers and ceramic particles [1]. Most of the time, the particulate composites are developed with the addition of particulates externally.

Out of all the available processing techniques, most of the techniques used the mixing of matrix and reinforcement to develop composite. Due to the negative pressure difference, the externally attached liquid particles are strained. The vortex present also draws the air bubble, which causes the porosity in the casted composite. There are two ways of adding particulates (i) the addition of particulates above the liquidus temperature; (ii) In semi-solid slurry, the particulates are added in the compo-casting temperature range [2]. In both of the methods mentioned above, the vortex technique

is used. The closeness of ceramic particles in the matrix material affects the tribological characteristics. Hard particles like Al_2O_3, SiC, Si_3N_4, etc., decrease the wear rate and improve the mechanical properties compared to the base alloys [2, 3]. The shape and size of particles in the composite play a pivotal role in the characteristics of the developed composite. It has been observed from the previously published research that the WR significantly reduces with the increase in hard-phase volume fraction and particle size [4-6]. In dry sliding wear, the wear behaviour of the developed composite relies on many factors like volume fraction, dispersed stages and size [7, 8], abrasive size [7, 9, 10], abrasive load applied [2, 7] and rake angle [7]. Researchers investigated the wear behaviour of Al-Si alloy with/without the addition of 3% alumina [11]. The wear resistance significantly decreases at a load of 1MPa for the developed composite. In another experiment conducted by researchers [12, 13] on lower and higher percentage alumina reinforced composite, it was found that the higher amount of resistance and ductility. After the 15% addition of Al_2O_3, the tensile strength decreases due to the agglomeration of the particulate. The morphological investigation of the developed composite revealed that the particles are uniformly distributed in stir casting, which reflects a great bonding among the ceramic particles and matrix material.

The characterization envisaged that the properties depend upon the reinforcement type, their bonding, and size [14]. Researchers developed the composite using SiC and graphite and tested the developed composite by dry sliding wear. It was found that the graphite-based composite shows a significantly low amount of wear rate as compared to the SiC-based composite [15, 16]. In another research on a dry sliding wear testing machine after varying the sliding velocity (1.25 to 3.05 m/s), load (10-50 N), and sliding distance (0.5 to 3 km) [17]. It was investigated that an increment in the weight

percentage of alumina in AA2014 increases the wear resistance in dry sliding [4]. The lubrication characteristics were incorporated into the composite after adding graphite [18, 19]. The tribological behaviour was significantly enhanced after the inclusion of particulate. However, a small change in the mechanical properties was observed. The anti-seizing characteristics were improved after incorporating self-lubricating materials like graphite or mica; however, abrasion resistance is improved after including hard particles like SiC, alumina, B_4C, Si_3N_4, etc. [20-22].

A recent study by Patil et al. (2024) investigated the use of fly ash and SiC as hybrid reinforcements in aluminium composites, reporting significant improvements in wear resistance and hardness [23]. Similarly, Bologun et al. (2022) explored the tribological behaviour of aluminium composites reinforced with waste glass particles, demonstrating a 30% reduction in wear rate compared to conventional composites [24]. Another study by Ventura et al. (2022) highlighted the potential of using recycled carbon fibers from industrial waste as reinforcements, achieving a 25% improvement in tensile strength and wear resistance [25].

Despite these advancements, limited research has been conducted on the use of lignocellulosic waste materials, such as lignocellulosic solid waste (LSP), as reinforcements in aluminium composites. A recent study by Narendran et al. (2023) explored the mechanical properties of aluminium composites reinforced with coconut shell ash, reporting a 20% increase in hardness and wear resistance [26]. However, the tribological performance of Al/LSP composites under varying wear conditions remains unexplored, presenting a significant research gap [27].

It is clear from the literature that the developed composite exhibits better tribological characteristics than the alloys. Therefore, composites have several applications in

automobile and aerospace industries, especially in wear-prone areas. From the literature, limited work has been observed on industrial waste like LSP. Thus, in the current work, an effort has been made to develop Al/LSP composite by stir-casting technique. The developed composite has been characterized by various combinations of input parameters. To verify the applications of the developed composite regarding the seizure or scuffing resistance in the tribological system, it is mandatory to check the developed composite against the criteria mentioned earlier. Therefore, the developed composite is checked in the following two areas:

(i) The influence of the weight percentage of LSP on the tribological behaviour

(ii) Investigation of WR and CF on Al/LSP composite at various wear conditions

(iii) Implementation of GRA on the performance characteristics and investigation of the best wear condition to minimize the WR.

2. Materials and methods

2.1. Matrix material and reinforcement

The matrix material used in this work is Al-Si-Mg alloys, which have good corrosion resistance and castability. Due to these characteristics, these alloys have applications in connecting rods, cylinder liners, brake drums, etc. Industrial waste (limestone powder) is used as a reinforcement for the development of composite. The limestone powder (LSP) is collected from the stone processing industries. Thus, using industrial waste in composite materials goes towards sustainable development by reducing the adverse effects on the environment. LSP is dried for 15 days and heated for 3 hrs at 300°C. The matrix material is cut into small pieces and then preheated for 1 hour at a temperature of 300°C. The matrix material and reinforcement are put

together in the muffle furnace, and the stirrer is rotated at a constant speed of 300 RPM at a temperature of 800°C. Figure 1 illustrates the XRD analysis of LSP, which reveals its composition. The analysis shows that LSP primarily consists of calcite ($CaCO_3$), with minor quantities of dolomite ($Mg(CaCO_3)_2$) and quartz (SiO_2). This information is crucial for understanding the material properties and their influence on the composite. The presence of calcite contributes to improved load-bearing capacity, while dolomite and quartz enhance hardness and wear resistance. These characteristics make LSP a suitable reinforcement material for composites, providing improved mechanical and tribological properties.

Figure 1. XRD of the developed composite.

Figure 2. Sequence of Processes in the present work.

Figure 2 shows the sequence of processes adopted in the current research, which includes the raw material for composite development. The stir-casting process has been adopted for the composite development. Then, the wear rate and coefficient of friction are evaluated using a pin-on-disc apparatus. Both responses are analysed and interpreted.

2.2. Recording of response variables

In the present work, WR and CF are the responses considered for analysis. A wear test is performed on the Ducom TR-20 pin-on-disc apparatus. The coefficient of friction (CF) is directly measured from the display. However, the wear rate (WR) is measured from the loss of mass and Eq. 1. The specimens are extracted from the developed composite. The specimen is 6 mm in diameter and 27mm in length (ASTM G-99-95). All the specimens were polished before the wear test. The pin's weight is measured before and after the wear test in 'g' using a weighing balance. The counter surface is

made of EN31 hardened steel and cleaned with acetone after each run. Eq. 1 is used to measure wear rate (WR) in mm^3/m.

$$WR = \frac{\Delta m / \rho}{V.t} \quad (1)$$

Here, WR- Wear rate (WR) in (mm^3/m), Δm - loss of mass in (g), V- sliding velocity (m/s), ρ - density (g/cm^3); t-test duration (s).

2.3.Experimental array and level of parameters

The experiments are performed based on Taguchi's L_{25} orthogonal array in the present work. The steady-state wear rate and coefficient of friction were determined for different boundary conditions and Taguchi L_{25} orthogonal array design of experiment methodology was used to determine the effect of input control parameters on the output wear rate and coefficient of friction variables. Performance characteristics are determined through the S/N ratio and smaller-the-better criteria are suggested as the least wear rate and least coefficient of friction are desirable for best tribological performance.

The four control parameters viz., load (L), reinforcement weight% of LSP (R), sliding distance (D), and sliding velocity (V), at 5 levels are shown in Table 1. The process parameters and their levels are selected after performing preliminary experiments.

Table 1. Levels of Control Parameters for Taguchi L_{25}.

The tribological parameters are determined for a load range of 10–50 N, wt.% LSP range of 0–16%, sliding distance of 500–2500 m, and sliding velocity range of 0.5–2.0 m/s with an increment of 0.375 m/s at each level. The experiments are conducted in random order and the results are depicted in supplementary Table S1 to

Table S6. Table 1 shows the values of the different levels of the 4 control parameters, which are to be used in the L_{25} design.

3. Methodology

The methodology adopted in the current work is presented in Figure 3, which describes the work divided into four steps.

The first step develops the experimental layout using a Taguchi-based L_{25} orthogonal array. All experiments were performed as per the experimental layout, and the responses (WR and CF) were recorded. In the second step, the GRA is applied, which includes data pre-processing, deviational sequence, calculation of grey coefficients, and grade values. In the next step, the ANOVA is implemented on the grade values, keeping the reinforcement, load, sliding distance and sliding velocity as input parameters. Further, the optimized setting of the input parameters is investigated considering grade values as response parameters. At the suggested setting of input parameters, the responses are initially predicted and then experimentally evaluated. The percentage error is computed between the predicted result and experimental values at the suggested optimized setting.

Figure 3. Proposed methodology in the present research.

4. Results and discussion

The experimental values of WR and CF corresponding to L_{25} OA are depicted in Table 2.

Table 2. L_{25} Experimental layout.

A grey system is a system where some information is known, and some information is unknown. When complete information is known, that system is termed white; when the complete information is unknown, it is termed a black system. However, when we have some set of known information and some set of unknown

information, then it is known as a grey system. The ideal situations never exist in the real-world problem. Here, we always deal with the extremes of black and white, which are grey, fuzzy or hazy. There is always some uncertainty between the middle of extremes or in the grey area. Therefore, the lack of information in the system is completed from black to white through grey. Thus, the grey analysis provides a complete set of solutions to a problem where only some of the information is available, and others still need to be discovered. In this approach, one solution is completely undefined (namely '0'), and for one solution, all information is perfectly available (with a distinct solution, namely '1'). The number of solutions between these two varies from 0 to 1.

The grey analysis can precisely handle the problems that are unclear or incomplete information is available. The applications of grey relational analysis are found in performance evaluation, prediction analysis, project selection, the effect of factors on response, etc. Numerous researchers implemented grey theory to optimize the process performance associated with multiple responses using the grade values [28].

4.1. Steps Involved in Grey Relational Analysis

The use of the Taguchi method with GRA to optimize the tribological responses with multiple response characteristics involves the following steps [29]:

- Identify the process parameters and tribological responses to be determined.
- Determine the different levels of the input parameters.
- Choose the appropriate design of experiments (DOE) and designate the process parameters to the OA.
- Perform the experiments based on the arrangement of the OA.
- Normalize the experiment results.

- Calculate the GRC.
- Calculate the GRG by averaging the grey relational coefficient.
- Perform ANOVA on grade to determine the significance of process parameters.
- Perform Response Surface Regression on GRG.
- Conduct Response Surface Optimization on GRG.

4.2.Multi-response optimization using GRA

To optimize multi-responses effectively, GRA is used. Therefore, it is essential to transform multiple responses into an equivalent single response to achieve the best optimal parameter setting. In the GRA, WR and CF responses are initially normalized between {0 and 1} to reduce inconsistency. Using smaller-the-better criterion by Equation 2.

$$X_i(k) = \frac{max\, y_i(k) - y_i(k)}{max\, y_i(k) - min\, y_i(k)} \tag{2}$$

where, $X_i(k)$ are the normalized grey relation values for the k^{th} response, $max\, y_i(k)$ and $min\, y_i(k)$ are the greatest and least values of $y_i(k)$ for k^{th} response. For experimental runs (i =1, 2 ... n) and factors (k =1, 2 ... k).

The GRC (ξ) is calculated as follows:

$$\xi_i(k) = \frac{\Delta_{min} + \varsigma\Delta_{\max}}{\Delta_{oi}(k) + \varsigma\Delta_{max}} \tag{3}$$

Where $\Delta_{oi}(k)$ is the deviation sequence from the reference sequence, which may be computed by taking the difference among $x_o(k)$ and $x_i(k)$. The distinguishing coefficient (ς) value is assumed based on distinguished ability. Usually, the distinguishing coefficient (ς) value is considered 0.5.

$$\Delta_{oi}(k) = \| x_o(k) - x_i(k) \| \tag{4}$$

$$\Delta_{min} = \min_{\forall i \in n} \min_{\forall k} \left| x_0(k) - x_i(k) \right| \quad (5)$$

$$\Delta_{max} = \max_{\forall i \in n} \max_{\forall k} \left| x_0(k) - x_i(k) \right| \quad (6)$$

Therefore, the GRG may be determined by the average of GRC for each response.

$$\gamma_i = \frac{1}{n} \sum_{k=1}^{n} W_i \xi_i(k) \qquad where \sum_{k=1}^{n} W_i = 1 \quad (7)$$

The GRG value indicates the overall performance index.

4.3.GRG calculations

The values of wear rates of Taguchi L_{25} design for Al-LSP composite, Normalized WR rates, Deviation Sequence for WR, and GRC for WR are shown in Table 3. Further, the maximum, minimum and mean values of each column are used in the computation of GRC and grade, as shown in Table 3.

Table 3. GRC and Grade Calculations for WR and CF.

Deviation Sequence values are obtained by subtracting normalized values from 1.

$$Deviation\,Sequence = 1 - Normalized\,Value \quad (8)$$

It is because of this inversion, maximum GRC corresponds to minimum WR. Since the deviation sequence is inverted here, maximum GRC corresponds to the minimum CF. After calculating individual GRC for WR and CF, the composite grade is determined by using the following formula.

$$GRG = 0.5 \times GRC_{WR} + 0.5 \times GRC_{CF} \quad (9)$$

In this research work, both WR and CF are assigned equal weights (W_{WR} = 0.5, W_{CF} = 0.5), as optimization is performed without being application-specific.

Table 3 lists the overall Grey Relational Grade value along with its rankings. GRG with maximum value is assigned Rank 1, and subsequent rankings are assigned in the descending order of GRG values.

Table 3 shows that the highest GRG (0.956) value is obtained for experimental run 5 ranked with 1 representing the best-combined performance of wear rate and coefficient of friction. Run 22 represents the least combined performance with a GRG (0.360) value with a rank of 25.

The influence of different control parameters on GRG is shown in a response table. The response table is tabulated for different levels of parameters by determining the average value grey grade and is shown in Table 4.

Table 4. Response Table of GRG.

The influence of different parameters at every level is shown in Table 4. From Table 4, it can be inferred that the load is the most influential parameter on GRG, with the highest delta value, followed by sliding distance, % LSP, and sliding velocity.

Figure 4. Response graphs of GRG.

Figure 4 shows the main effects plot for means for GRG in terms of control parameters (L, R, D, V).

The response graph for GRG reveals that load (L) is the most influencing factor at level 1 (10N), followed by % of LSP (R) at level 4 (12%), and sliding distance (D) at level 5 (2500 m) as well sliding velocity (V) at level 5 (2 m/s), referring to the highest average grey relational grade. GRG's optimal parameter combination is L_1 R_4 D_5 V_5 (L-10 N, R-12%, D-2500 m, V-2.0 m/s).

4.4.ANOVA of GRG

Analysis of variance (ANOVA) is computed to determine the ranking order of significance of the control parameters on the GRG for the Al-LSP composites.

ANOVA is performed to reveal the significance of control parameters on the response CF.

Table 5. ANOVA of GRG.

From the ANOVA (Table 5), it is determined that the load (63.4%, p = 0.000 < 0.05) is the most critical parameter, followed by sliding distance (21.1%, p = 0.000 < 0.05) and % of LSP (13.9%, p = 0.000 < 0.05). The sliding velocity (0.4%, p = 0.678 > 0.05) is insignificant on the grey relational grade.

4.5.Response Surface Regression Modelling of GRG

The model adequacy is investigated with the help of residual plots, which are shown in Figure 5.

Figure 5. Residual Plots of Grey Relational Grade.

Figure 5 suggests that the residuals follow a normal distribution and satisfy the conditions of randomness and independence of each other.

Using linear regression, the GRG model is developed in terms of control parameters: load *(L)*, % of LSP, sliding distance *(D)*, and sliding velocity *(V)*.

$$\underset{(94.10\%)}{GRG} = 0.5914 - \underset{(60.19\%)}{0.008253L} + \underset{(11.52\%)}{0.00903R} + \underset{(21.34\%)}{0.000098D} + \underset{(1.05\%)}{0.0290V} \quad (10)$$

The GRG value is directly proportional to % of LSP (R), sliding distance (*D*) and sliding velocity *(V)* and inversely proportional to load *(L)*. Further, load is the most important parameter on GRG, followed by sliding distance, wt% LSP. The effect of sliding velocity on GRG is insignificant.

5. Response Surface Optimization of GRG

Response surface optimization is conducted on Grey Relational Grade to evaluate the optimum control parameter settings that yield maximum Grey Relational

Grade. The optimization problem of maximizing Grey Relational Grade can be stated as

$$Objective\,Function: Maximize\left(GRG\right) 0.5914 - 0.008253L + 0.00903R + 0.000098D + 0.0290V \quad (11)$$

Constraints: No Constraints

$$Design\,Variables\,Bounds: 10 \le L \le 50, 0 \le R \le 16, 500 \le D \le 2500, 0.5 \le V \le 2.0 \quad (12)$$

As a starting point for the optimization, the point with maximum Grey Relational Grade in the L_{25} experiments are specified: (Exp No. 5) *L = 10, R = 16, D = 2500, V = 2.0*. After several iterations, MINITAB found the maximum Grey Relational Grade point as *L = 10 N, R = 16%, D = 2500 m, V = 2.0 m/s*, and maximum Grey Relational Grade = 0.957.

Figure 6. Contour plots between the GRG and input process parameters.

Figure 6 (a-f) depicts the counterplot between the grade values and input process variables. The counter plots define the relationship of input parameters with the grey grade by colour coding. The range of colour code is already provided in the inset of Figure 6 (a-f). The high grey grade values are preferred for better performance characteristics. Therefore, the purple colour presents grey grade values greater than 0.9, and the corresponding values of input parameters are adjusted to set suitable wear conditions. From every Figure, it is evident that a low value of load, and the high value of reinforcement, velocity and distance are preferred for high grade.

Table 6. Confirmation results at the Optimized Setting.

Table 6 provides the confirmation experiment results, predicted value and comparison of the rank 1 experimental setting from 25 experiments and the optimized setting investigated from analysis. The rank 1 experimental setting is L: 10 N; R: 16%; D: 2500 m and V: 2 m/s; however, the optimized setting from the analysis is L: 10 N; R:

12%; D: 2500 m and V: 2 m/s. The comparison between the performance characteristics in both cases has been made, and it has been observed that the WR increases by 4.67%. However, an improvement of 24.83% has been found for CF.

Figure 7. EDAX of Worn Surface of Al-12%LSP composite.

The EDAX analysis reveals Fe and O in the surface, confirming the formation of a Mechanically Mixed Layer (MML) on the worn surface (Figure 7).

Figure 8. Microstructure of the developed composite at (a) 12% LSP and (b) 16% LSP.

Figure 9. SEM Images of Worn-out Surface for (a) Al-Alloy (b) Al-4%LSP (c) Al-8%LSP (d) Al-12%LSP.

Figure 8 shows the microstructure of the developed composite for 12% and 16% LSP addition in the Al-alloy. Figure 9 represents the worn-out surfaces of Aluminium alloy and Al-LSP composites (developed with different reinforcement percentages) using a Scanning Electron Microscope (SEM). Figure 9 presents the micro-cutting, particle pull-out and deep grooves at different reinforcement percentages. Figure 9a depicts the SEM micrograph of Al-alloy, which shows the micro-crack and some pull-out material, which appears due to the movement of the pin on the counter surface. The formation of cracks is due to the alteration in the CF values during the wear test. Figure 9b shows an SEM micrograph of the worn-out surfaces of the 4% LSP reinforcement composite. The worn-out surface shows that the plastic deformation decreases as compared to base-alloy. With the addition of more reinforcement (8% LSP), the material became thermally stable, which can be observed in Figure 9c. The worn-out surface after 12% LSP addition was depicted in Figure 9d, which shows that the surface quality is improved than the lower reinforcement percentage, and indicates some improvement in surface features of aluminium with 12% wt. of LSP composite.

The surface is much smoother, has fewer depth of cuts and is finer. As reinforcement increases, the al-composite becomes thermally stable, which makes the surface much harder due to strain hardening. The addition of reinforcement decreases the CF, which protects the developed composite from raising the temperature and maintains a low coefficient of thermal expansion.

6. Conclusions

Industrial waste (LSP) has become an issue for the environment. Therefore, the use of LSP for the fabrication of composites is a mark of the sustainable development of the composite material. The characterization of the developed composite was completed using the grey approach. Both the tribological performance characteristics (WR and CF) are combined into a single tribological index called GRG using GRA. The conclusions from the present work are summarized below:

1. The optimal parameter combination that results in maximum GRG is L_1 R_4 D_5 V_5 (L:10 N, R:12%, D: 2500 m, V: 2.0 m/s).
2. The ANOVA reveals that L has the maximum influence (63.4%) on grade value followed by D (21.1%) and R (13.9%).
3. GRG of Al-LSP is directly proportional to the reinforcement percentage of LSP and sliding distance, and inversely proportional to load. Therefore, the grade value increases with the increase in reinforcement percentage and D, while the grade value decreases with the increase in L.
4. After implementing the grey approach, the wear rate increases by 4.67%, while CF decreases by 24.83%. Thus, a significant improvement in the tribological characteristics of the Al/LSP composite can be obtained after the grey approach.

5. The SEM micrograph shows that at the optimized setting of reinforcement percentage of LSP, the material becomes thermally stable, which makes the worn-out surface much smoother.

Funding

This research did not receive any specific grant from funding agencies in the public, commercial, or not-for-profit sectors.

Conflicts of interest

The authors declare that they have no known competing financial interests or personal relationships that could have appeared to influence the work reported in this paper.

Authors contribution statement

Neeraj Sharma: Writing original draft, Ideology, Formulation,

Dharmana Lokanadham: Experimentation, data collection, formulation

Rakesh Chandmal Sharma: Analysis

Srihari Palli: Writing, review and editing

K. Venkatasubbaiah: Supervision, conceptualization

B. V. Ramana: Writing, Review and Editing

The supplementary data is available at:

file:///C:/Users/pc/Downloads/Supplementary-%20Lokanadham%20(40-SCI-2409-9451%20)%20(1).pdf

References

1. Dang, W., Wang, W., Wu, P., et al. "Freeze-cast porous Al_2O_3 ceramics strengthened by up to 80% ceramics fibers." *Ceramics International*, *48*(7), pp. 9835-9841 (2022). http://doi.org/10.1016/j.ceramint.2021.12.185
2. Nagaral, M., Deshapande, R.G. Auradi, V., et al. "Mechanical and Wear Characterization of Ceramic Boron Carbide-Reinforced Al2024 alloy Metal Composites." *J. Bio-and Tribo-Corrosion,* 7, pp. 1–12 (2021). http://doi.org/10.1007/s40735-020-00454-8
3. Arya, R.K., Kumar, R., Telang, A., et al. "Effect of Microstructure on Mechanical Behaviors of Al6061 Metal Matrix Composite Reinforced with Silicon Nitride (Si3N4) and Silicon Carbide (SiC) Micro Particles," *Silicon*, *15*(14), pp. 5911-5923 (2023). http://doi.org/10.1007/s12633-023-02468-6
4. Stephens, J.J., Lucas, J.P. and Hoskingm, F.M. "Cast Al-7 Si Composites: Effect of Particle type and size on Mechanical Properties." *Scr. Metall.* 22, pp. 1307–1312 (1988). http://doi.org/10.1016/S0036-9748(88)80152-2
5. Bagheri, B., Shamsipur, A., Abdollahzadeh, A., et al. "Investigation of SiC

nanoparticle size and distribution effects on microstructure and mechanical properties of Al/SiC/Cu composite during the FSSW process: experimental and simulation," *Metals and Materials International*, *29*(4), pp. 1095-1112 (2023).
http://doi.org/10.1007/s12540-022-01284-8

6. Dong, B.X., Li, Q. Y., Shu, S.L., et al. "Investigation on the elevated-temperature tribological behaviors and mechanism of Al-Cu-Mg composites reinforced by in-situ size-tunable TiB2-TiC particles,' *Tribology International*, *177*, article ID 107943 (2023).
http://doi.org/10.1016/j.triboint.2022.107943
7. Prasad, B.K., Das, S., Jha, A.K., et al. "Factors Controlling the Abrasive Wear Response of a Zinc-based Alloy Silicon Carbide Particle Composite." *Compos. Part A Appl. Sci. Manuf.* 28, pp. 301–308 (1997).
http://doi.org/10.1016/S1359-835X(96)00115-7
8. Bharath, V., Auradi, V., Nagaral, M., et al. "Microstructural and wear behavior of Al2014-alumina composites with varying alumina content." *Transactions of the Indian Institute of Metals*, pp. 1-15 (2022).
http://doi.org/10.1007/s12666-021-02405-4
9. Dwivedi, S.P., Sharma, S., Li, C., et al. "Effect of nano-TiO2 particles addition on dissimilar AA2024 and AA2014 based composite developed by friction stir process technique," *Journal of Materials Research and Technology*, *26*, pp. 1872-1881 (2023).
http://doi.org/10.1016/j.jmrt.2023.07.234
10. Sannino, A.P. and Rack, H.J. "Dry Sliding Wear of Discontinuously Reinforced Aluminum Composites: Review And Discussion," *Wear*. 189,

pp.1–19 (1995).

http://doi.org/10.1016/0043-1648(95)06657-8

11. Vencl, A., Bobić, I., Jovanović, M.T., et al. “Microstructural and tribological properties of A356 Al–Si alloy reinforced with Al_2O_3 particles.” *Tribology Letters*, *32*, pp. 159-170 (2008).

http://doi.org/10.1007/s11249-008-9374-6

12. Sajjadi, S.A., Ezatpour, H.R. and Parizi, M.T. "Comparison of Microstructure and Mechanical Properties of A356 Aluminum Alloy/Al_2O_3 Composites Fabricated by Stir and Compo-Casting Processes." *Mater. Des.* 34, pp. 106–111 (2012).

http://doi.org/10.1016/j.matdes.2011.07.037

13. Murthy, B. V., Auradi, V., Nagaral, M., et al. “Al2014–alumina aerospace composites: particle size impacts on microstructure, mechanical, fractography, and wear characteristics,” *ACS omega*, *8*(14), pp. 13444-13455 (2023).

http://doi.org/10.1021/acsomega.3c01163

14. Li, X.Y. and Tandon, K.N. "Microstructural Characterization of Mechanically Mixed Layer and Wear Debris in Sliding Wear of an Al Alloy and an Al based Composite." *Wear* 245, pp.148–161(2000).

http://doi.org/10.1016/S0043-1648(00)00475-0

15. Chandel, R., Sharma, N. and Bansal, S.A., “A review on recent developments of aluminum-based hybrid composites for automotive applications.” *Emergent Materials*, *4*(5), pp. 1243-1257 (2021).

http://doi.org/10.1007/s42247-021-00186-6

16. Basavarajappa, S., Chandramohan, G. and Davim, J.P. "Application of Taguchi Techniques to Study Dry Sliding Wear Behaviour of Metal Matrix

Composites", Mater. Des. 28, pp.1393–1398(2007).
http://doi.org/10.1016/j.matdes.2006.01.006

17. Sharma, S.C. "The Sliding Wear Behavior of Al6061–Garnet Particulate Composites." Wear. 249, pp.1036–1045 (2001).
http://doi.org/10.1016/S0043-1648(01)00810-9
18. Nikhil, G. Ji and Prakash, R. "Hydrothermal Synthesis of Zn-Mg-Based Layered Double Hydroxide Coatings for the Corrosion Protection of Copper in Chloride and Hydroxide Media." *Int. J. Miner. Metall. Mater.* 28, pp.1991–2000 (2021).
http://doi.org/10.1007/s12613-020-2122-0
19. Kumar, N., Kumar, H.V., Raju, T.H., et al. "Microstructural characterization, mechanical and taguchi wear behavior of micro-titanium carbide particle-reinforced Al2014 alloy composites synthesized by advanced two-stage casting method." *Journal of Bio-and Tribo-Corrosion*, 8(4), pp. 109 (2022).
http://doi.org/10.1007/s40735-022-00709-6
20. Sahoo, B., Paul, J. and Sharma, A. "Mechanical and Tribological Behaviour of Surface-Graphitised Al-1100 Alloy." *Lubricants*, *12*(4), p. 139 (2024).
http://doi.org/10.3390/lubricants12040139
21. Arya, N.K., Sharma, R. Ullas, A.V, et al. "Synthesis of Chitosan/Nickel Oxide Nanocomposite for Corrosion Prevention of Copper in NaCl Solution." *Mater. Today Proc.*, 74, pp. 225–230 (2023).
http://doi.org/10.1016/j.matpr.2022.08.056
22. Wadhwa, A.S., & Chauhan, A. "An Overview of the Mechanical and Tribological Characteristics of Non-Ferrous Metal Matrix Composites for Advanced Engineering Applications." *Tribology in Industry*, 45(1), pp. 51-80

(2023).

http://doi.org/10.24874/ti.1359.08.22.12

23. Patil, N.A., Pedapati, S., & Pedapati, S.R. "Enhancing Wear Resistance of AA7075/SiC/Fly Ash Composites Through Friction Stir Processing." *Journal of Composites Science*, *8*(11), pp. 461 (2024). http://doi.org/10.3390/jcs8110461
24. Balogun, O.A., Akinwande, A.A., Adediran, A.A., et al. "Microstructure and particle size effects on selected mechanical properties of waste glass-reinforced aluminium matrix composites." *Materials Today: Proceedings*, *62*, pp. 4589-4598 (2022). http://doi.org/10.1016/j.matpr.2022.05.330
25. Ventura, A.M., Kneissl, L.M., Nunes, S., et al. "Recycled carbon fibers as an alternative reinforcement in UHMWPE composite. Circular economy within polymer tribology." *Sustainable Materials and Technologies*, 34, e00510 (2022). http://doi.org/10.1016/j.susmat.2022.e00510
26. Narendran, J., Nagaraja, S., Karthikeyan, T., et al. "Evaluation, tribological examination, and multi-objective optimization of aluminum-fly ash-egg shell composites for sustainability." *Engineering Reports*, *6*(12), e12980 (2024). http://doi.org/10.1002/eng2.12980
27. Dharmana, L., & Kambagowni, V.S. "Investigation of mechanical properties and tribological performance of Al-LSP and Al-Al2O3 composite." *World Journal of Engineering*, *19*(6), 766-776 (2022). http://doi.org/10.1108/WJE-03-2021-0172
28. Ahuja, N., Batra, U. and Kumar, K. "Multicharacteristics Optimization of

Electrical Discharge Micro Hole Drilling in Mg Alloy using Hybrid Approach of GRA–Regression–PSO." *Grey Syst. Theory Appl.* (2020). http://doi.org/10.1108/GS-03-2020-0029

29. Liu, S., Yang, Y., & Forrest, J.Y.L. "*Grey systems analysis: Methods, models and applications*." Cham: Springer (2022). http://doi.org/10.1007/978-981-19-6160-1

List of Figures:

List of Tables:

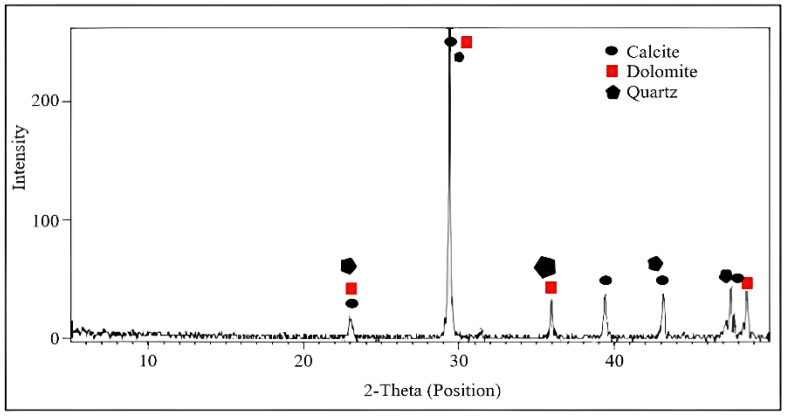

Figure 1. XRD of the developed composite.

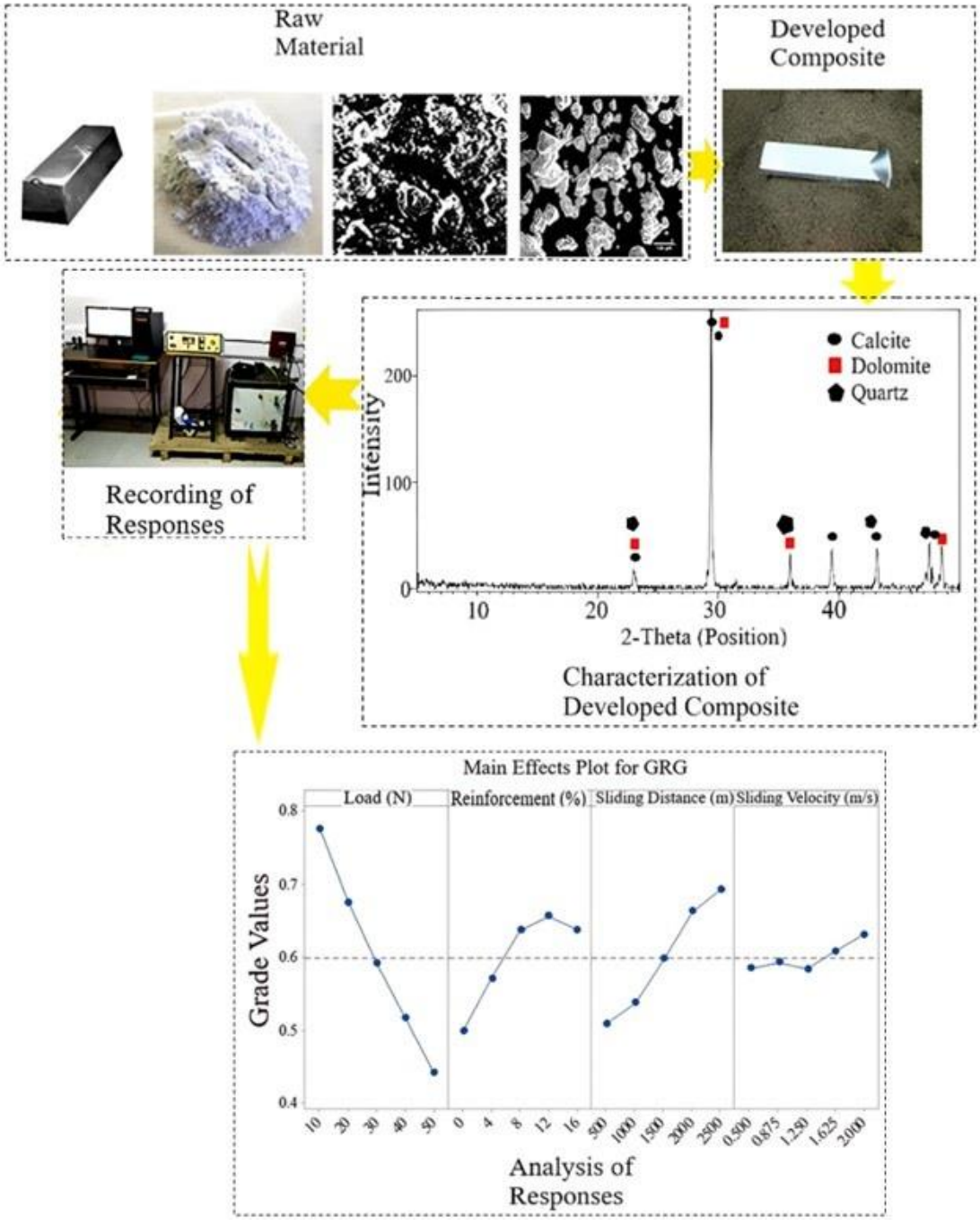

Figure 2. Sequence of Processes in the present work.

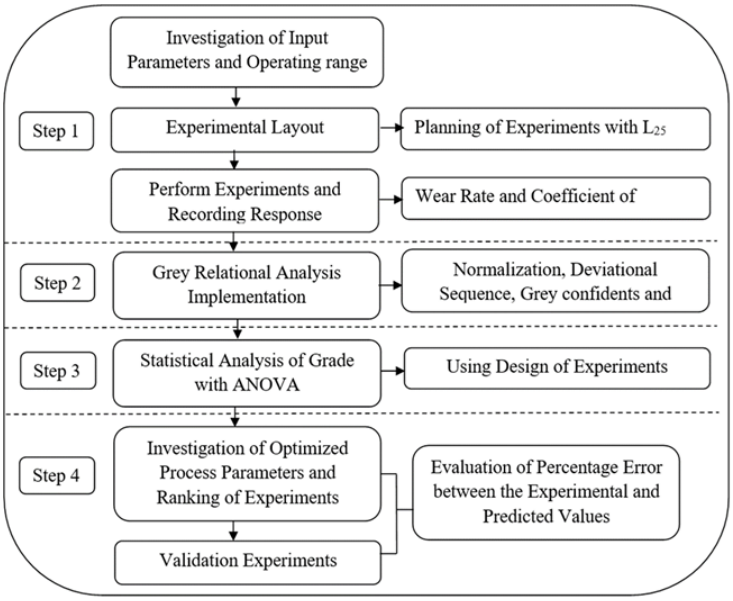

Figure 3. Proposed methodology in the present research.

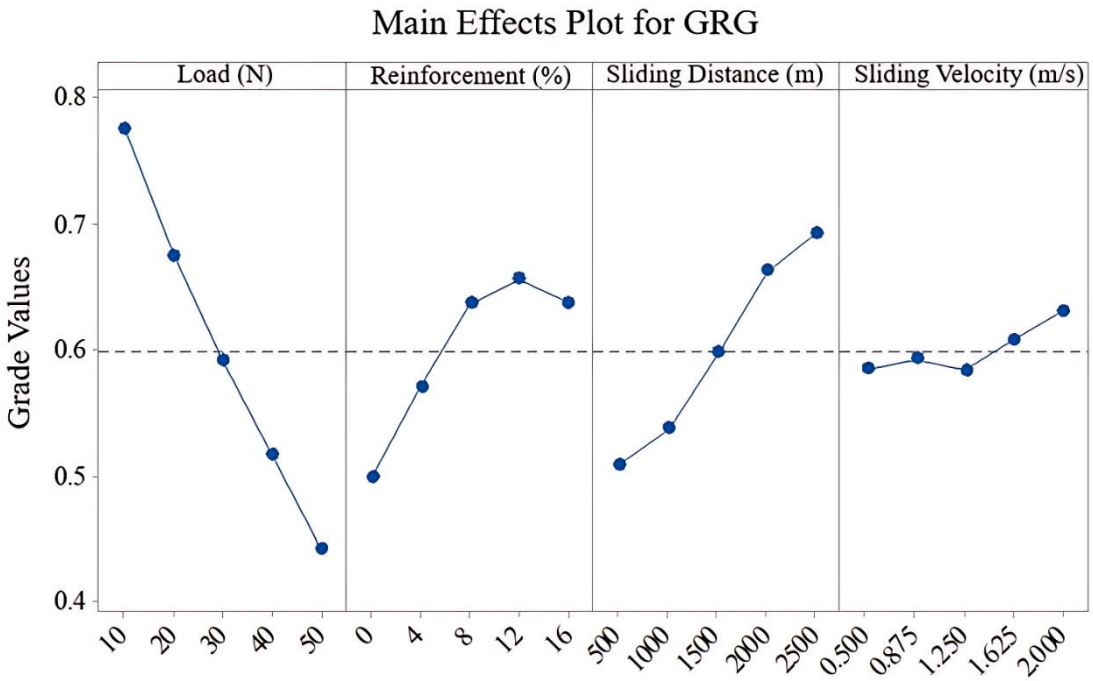

Figure 4. Response graphs of GRG.

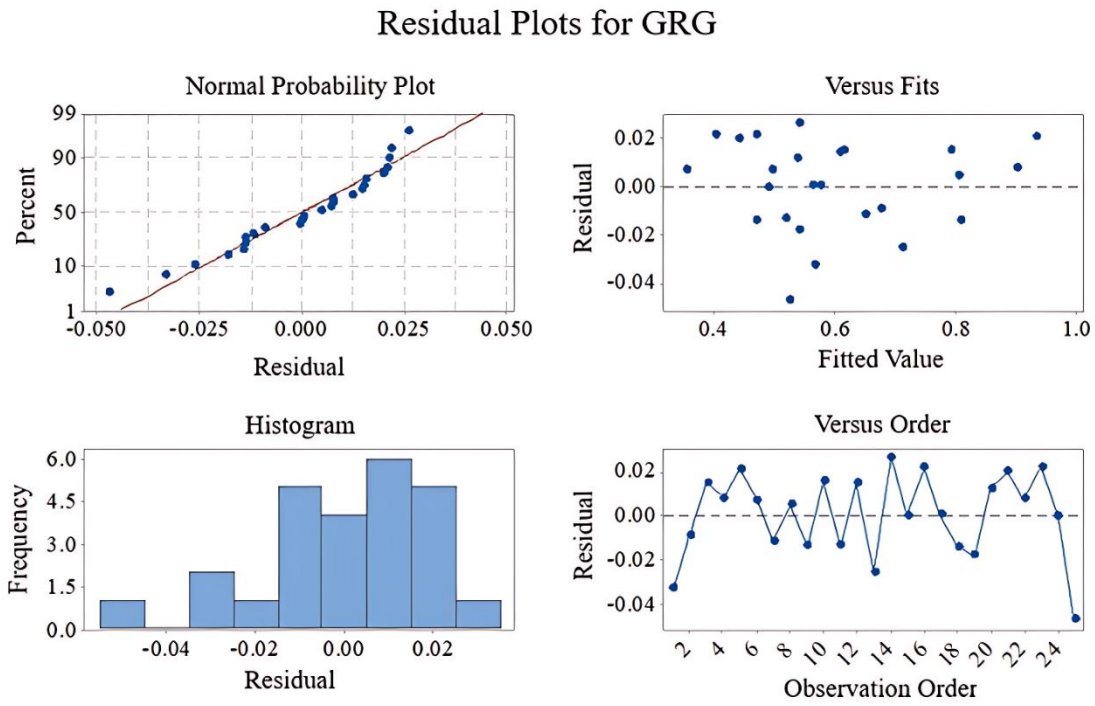

Figure 5. Residual Plots of Grey Relational Grade.

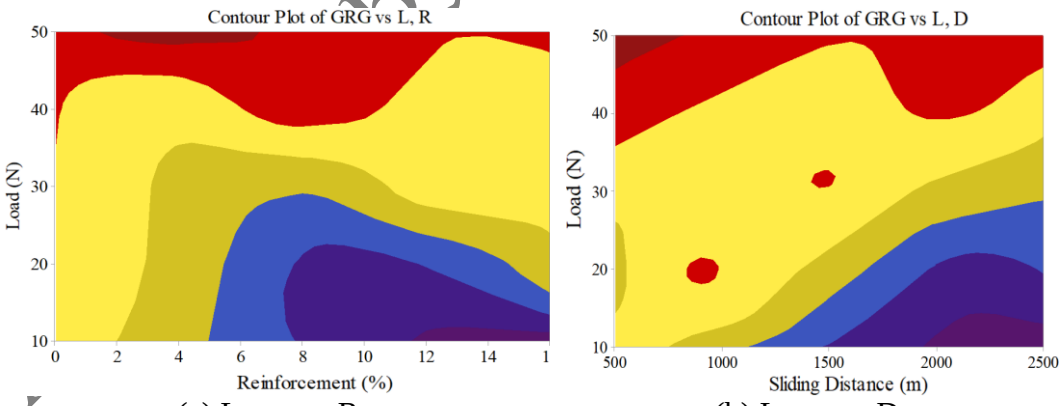

(a) L versus R (b) L versus D

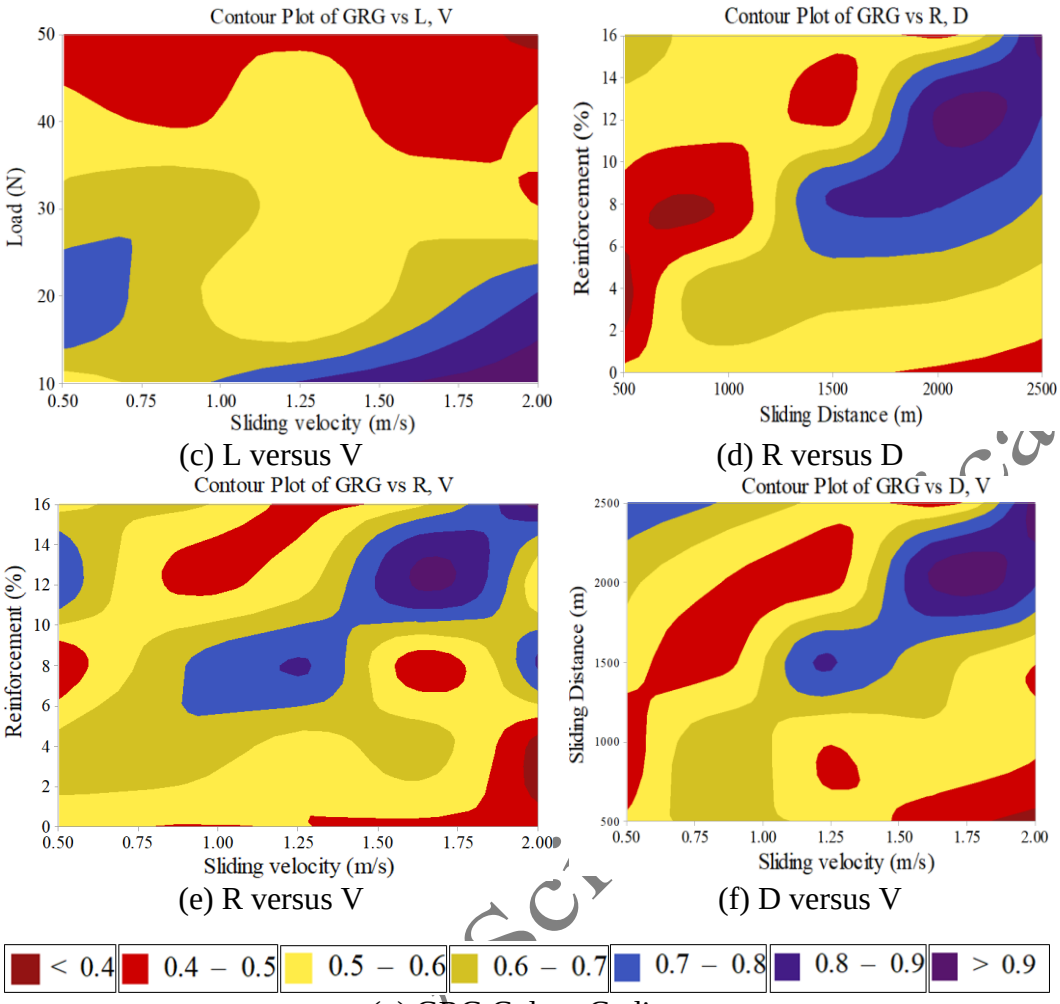

(c) L versus V (d) R versus D

(e) R versus V (f) D versus V

(g) GRG Colour Coding

Figure 6. Contour plots between the GRG and input process parameters.

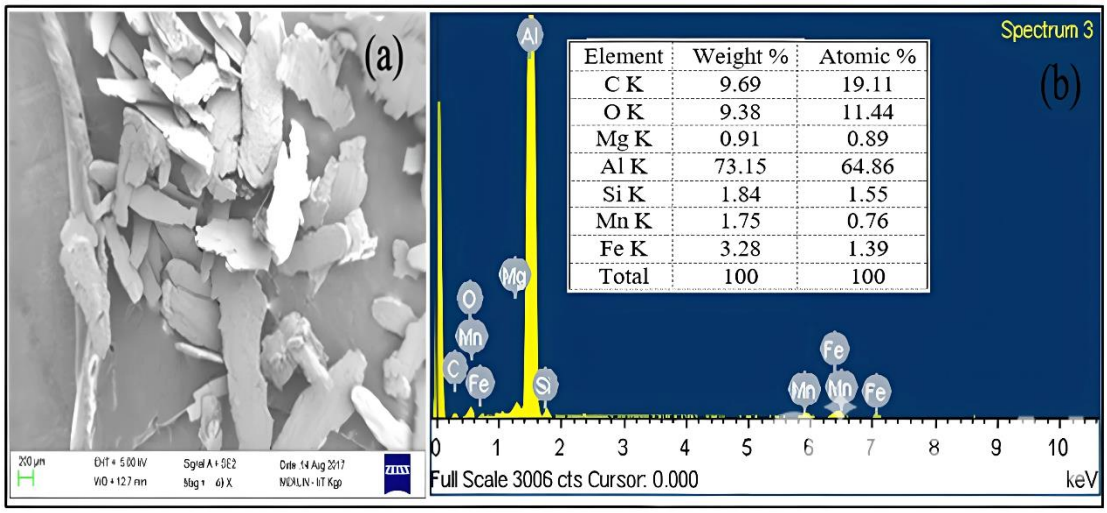

Figure 7. EDAX of Worn Surface of Al-12%LSP composite.

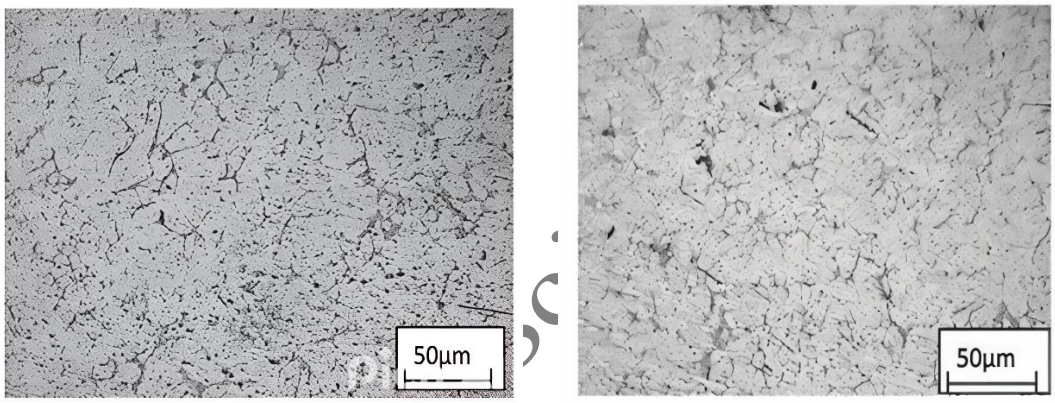

(a) (b)

Figure 8. Microstructure of the developed composite at (a) 12% LSP and (b) 16% LSP.

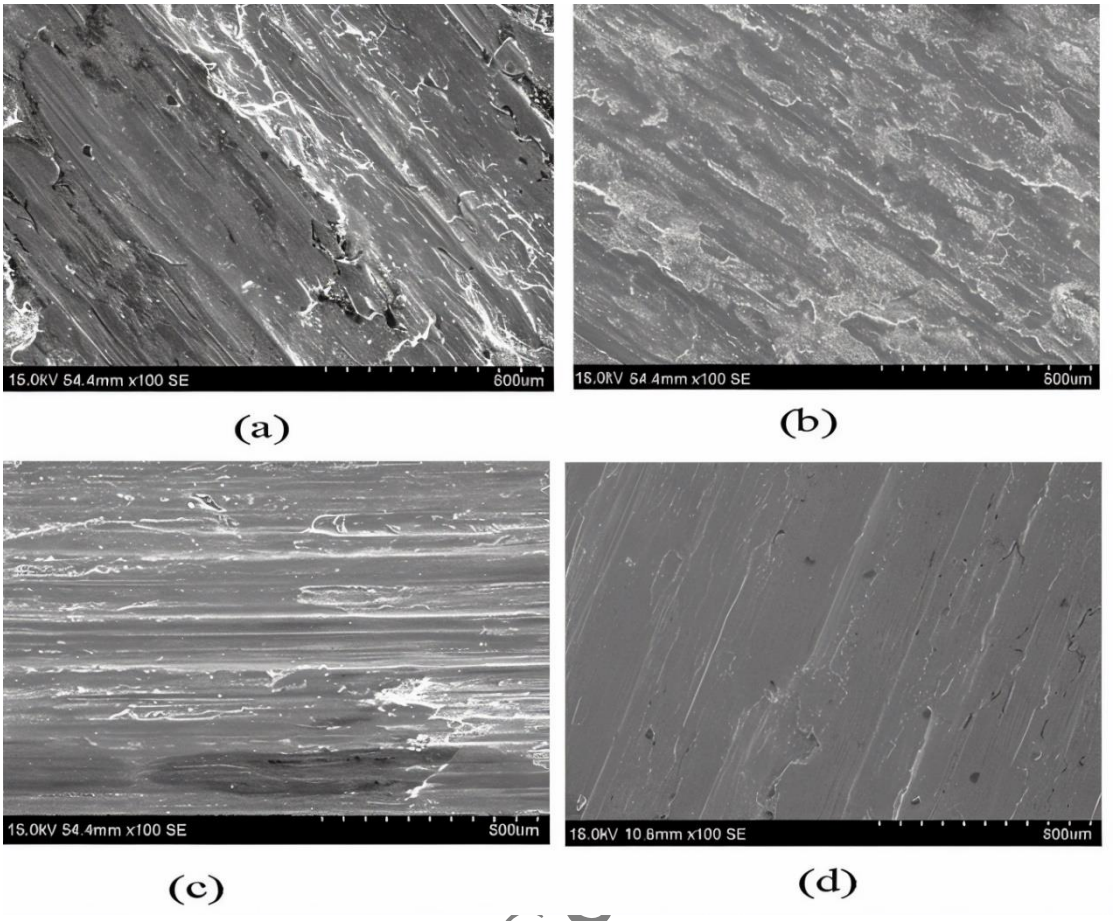

Figure 9. SEM Images of Worn-out Surface for (a) Al-Alloy (b) Al-4%LSP (c) Al-8%LSP (d) Al-12%LSP.

Table 1. Levels of Control Parameters for Taguchi L_{25}.

	Load 'L' (N)	Reinforcement 'R' (wt.%)	Sliding Distance 'D' (m)	Sliding Velocity 'V' (m/s)
Level 1	10	0	500	0.5
Level 2	20	4	1000	0.875
Level 3	30	8	1500	1.25
Level 4	40	12	2000	1.625
Level 5	50	16	2500	2

Table 2. L_{25} Experimental layout.

Exp. No	**Input Parameters**				**Responses**	
	Load (N)	**Reinforcement (%)**	**Sliding distance (m)**	**Sliding velocity (m/s)**	**WR (mm^3/m)**	**CF**
1	10	0	500	0.500	5.725	0.311

2	10	4	1000	0.875	4.482	0.230
3	10	8	1500	1.250	3.324	0.182
4	10	12	2000	1.625	2.252	0.168
5	10	16	2500	2.000	1.265	0.186
6	20	0	1000	1.250	5.480	0.363
7	20	4	1500	1.625	3.947	0.267
8	20	8	2000	2.000	2.500	0.205
9	20	12	2500	0.500	1.687	0.259
10	20	16	500	0.875	7.901	0.200
11	30	0	1500	2.000	4.586	0.412
12	30	4	2000	0.500	2.403	0.397
13	30	8	2500	0.875	2.576	0.294
14	30	12	500	1.250	8.660	0.229
15	30	16	1000	1.625	5.846	0.267
16	40	0	2000	0.875	3.682	0.540
17	40	4	2500	1.250	3.480	0.389
18	40	8	500	1.625	9.434	0.317
19	40	12	1000	2.000	6.245	0.308
20	40	16	1500	0.500	3.720	0.398
21	50	0	2500	1.625	4.399	0.543
22	50	4	500	2.000	10.222	0.466
23	50	8	1000	0.500	6.238	0.487
24	50	12	1500	0.875	4.760	0.436
25	50	16	2000	1.250	5.277	0.418

Table 3. GRC and Grade Calculations for WR and CF.

Exp. No.	**WR**	**CF**	**Normalized**		**Deviation Sequence**		**GRC**		**Grade**	**Rank**
			WR	**CF**	**WR**	**CF**	**WR**	**CF**		
1	5.725	0.311	0.502	0.619	0.498	0.381	0.501	0.567	0.534	15
2	4.482	0.23	0.641	0.835	0.359	0.165	0.582	0.752	0.667	7
3	3.324	0.182	0.77	0.963	0.23	0.037	0.685	0.931	0.808	4
4	2.252	0.168	0.89	1	0.11	0	0.819	1	0.9095	2
5	**1.265**	**0.186**	**1**	**0.952**	**0**	**0.048**	**1**	**0.912**	**0.956**	**1**
6	5.48	0.363	0.529	0.48	0.471	0.52	0.515	0.49	0.5025	18
7	3.947	0.267	0.701	0.736	0.299	0.264	0.625	0.654	0.6395	8
8	2.5	0.205	0.862	0.901	0.138	0.099	0.784	0.835	0.8095	3

9	1.687	0.259	0.953	0.757	0.047	0.243	0.914	0.673	0.7935	5
10	7.901	0.2	0.259	0.915	0.741	0.085	0.403	0.854	0.6285	9
11	4.586	0.412	0.629	0.349	0.371	0.651	0.574	0.435	0.5045	17
12	2.403	0.397	0.873	0.389	0.127	0.611	0.797	0.45	0.6235	10
13	2.576	0.294	0.854	0.664	0.146	0.336	0.774	0.598	0.686	6
14	8.66	0.229	0.174	0.837	0.826	0.163	0.377	0.755	0.566	12
15	5.846	0.267	0.489	0.736	0.511	0.264	0.494	0.654	0.574	11
16	3.682	0.54	0.73	0.008	0.27	0.992	0.649	0.335	0.492	19
17	3.48	0.389	0.753	0.411	0.247	0.589	0.669	0.459	0.564	13
18	9.434	0.317	0.088	0.603	0.912	0.397	0.354	0.557	0.4555	23
19	6.245	0.308	0.444	0.627	0.556	0.373	0.473	0.573	0.523	16
20	3.72	0.398	0.726	0.387	0.274	0.613	0.646	0.449	0.5475	14
21	4.399	0.543	0.65	0	0.35	1	0.588	0.333	0.4605	22
22	10.222	0.466	0	0.205	1	0.795	0.333	0.386	0.3595	25
23	6.238	0.487	0.445	0.149	0.555	0.851	0.474	0.37	0.422	24
24	4.76	0.436	0.61	0.285	0.39	0.715	0.562	0.412	0.487	20
25	5.277	0.418	0.552	0.333	0.448	0.667	0.527	0.429	0.478	21

Table 4. Response Table of GRG.

Level	L	R	D	V
1	0.7749	0.4987	0.5087	0.5841
2	0.6747	0.5707	0.5377	0.5921
3	0.5908	0.6362	0.5973	0.5837
4	0.5164	0.6558	0.6625	0.6078
5	0.4414	0.6368	0.6920	0.6305
Delta	0.3335	0.1571	0.1833	0.0468
Rank	1	3	2	4

Table 5. ANOVA of GRG.

Source	DF	SS	MS	F	P	% Contribution
L	4	68.763	17.191	103.60	0.000	63.4%
R	4	15.097	3.774	22.75	0.000	13.9%
D	4	22.904	5.726	34.51	0.000	21.1%
V	4	0.393	0.098	0.59	0.678	0.4%
Error	8	1.327	0.166			1.2%
Total	24	108.484	S = 0.4073	R-Sq = 98.8%	R-Sq(adj) = 96.3%	

Table 6. Confirmation results at the Optimized Setting.

Responses	$L_{10}R_{16}D_{2500}V_2$	$L_{10}R_{12}D_{2500}V_2$		Improvement (%)
	Experimental	Predicted	Experimental	
Grey Grade	0.957	0.95428	-	-
WR (mm^3/m)	1.265	1.364	1.327	-4.67
CF	0.186	0.15236	0.149	24.83

Biographies

Dr. Neeraj Sharma is currently working as an Associate Professor in Production Engineering Department of National Institute of Technology, Agartala, West Tripura (India). He has 14 years of teaching and research experience. His area of expertise is in the field of Biomaterials, composites, Smart materials, Non-Traditional Machining Processes and Additive Manufacturing. He has more than 100 peer-reviewed articles in journals and more than 35 articles presented in national and international conferences.

Dr. Dharmana Lokanadham received his M.Tech from Biju Patnaik University of Technology, Rourkela and Ph.D. from Andhra University, Visakhapatnam.His area of research is composite materials and Friction stir welding.He has 25 years of teaching experience.

Dr. Rakesh Chandmal Sharma received his MTech from Institute of Technology, Banaras Hindu University, Varanasi in 1998 and Ph.D. Indian Institute of Technology Roorkee in 2010. His area of research is vehicle dynamics and mechanical vibrations. He has 27 years of teaching experience.

Dr. Srihari Palli holds a Master's in Structural Dynamics from IIT Roorkee and a Ph.D. in Rail Vehicle Dynamics from Andhra University. He is associated with Technische University, Dresden, Germany for his Post Doctoral Research activities in the area of AI driven Rail Vehicle coupler systems. He has a total 22 years of academic, industrial and research experience.

Dr. K. Venkatasubbaiah received his M.Tech. and Ph.D. from Andhra University, Visakhapatnam. His area of research is supply chain management, materials and manufacturing. He has 30 years of teaching experience.

Bendi Venkata Ramana received his M.Tech from Jawaharlal Nehru Technological University, Kakinada and Ph.D. from Andhra University, Visakhapatnam. His area of research is Machine Learning. He has 23 years of teaching experience.